

- (14) Chavez, M.; Habichayn, P.; Maass, G.; Tsumura, R. *J. Chem. Eng. Data* 1986, 31, 218.
 (15) Lainez, A.; Gopal, P.; Zollweg, J. A.; Streett, W. B. *J. Chem. Thermodyn.* 1989, 21, 773.
 (16) Yokoyama, T.; Takahashi, S. *Proceedings of the 29th High Pressure Conference*, Fujisawa, Japan, The Japan Society of High Pressure Science and Technology: Fujisawa, Japan, 1988; p 116.
 (17) Jacobson, B. *Acta Chem. Scand.* 1952, 6, 1485.
 (18) Takagi, T.; Taranishi, H.; Yokoyama, C.; Takahashi, S. *Thermochim. Acta* 1989, 141, 291.

Received for review October 18, 1990. Revised March 22, 1991. Accepted May 13, 1991.

PVT and Vapor Pressure Measurements on 1,1-Dichloro-2,2,2-trifluoroethane (HCFC-123)

Chun-cheng Piao,* Haruki Sato, and Koichi Watanabe

Thermodynamics Laboratory, Department of Mechanical Engineering, Faculty of Science and Technology, Keio University, 3-14-1, Hiyoshi, Kohoku-ku, Yokohama 223, Japan

A complete set of *PVT* properties, vapor pressures, and critical parameters of 1,1-dichloro-2,2,2-trifluoroethane (HCFC-123) were measured by a constant-volume method. Values of 134 *PVT* property data were obtained along 19 isochores in a range of temperatures from 311 to 523 K, pressures from 0.5 to 12 MPa, and densities from 95 to 1440 kg·m⁻³, respectively. Results for 68 vapor pressures were obtained at temperatures from 308 K to the critical temperature, while a vapor pressure correlation representing the experimental data within ±0.26% was developed. The critical pressure was determined as 3.6655 ± 0.0030 MPa in the course of developing the vapor pressure correlation. The uncertainties of measurements are less than ±10 mK in temperature, ±2 kPa in pressure, and ±0.01 to ±0.14% in density, respectively. The purity of samples used was 99.8 and 99.82 wt %.

Introduction

1,1-Dichloro-2,2,2-trifluoroethane (HCFC-123, CHCl₂CF₃) is one of the promising substitutes for the conventional refrigerant CFC-11 (CCl₃F), but studies of the thermodynamic properties of HCFC-123 are rather limited, not only in the quantity of the reported data but also in the range of the measurements up to the present.

In the present study, the vapor pressures and *PVT* properties are reported in extensive temperature, pressure, and density range covering the entire fluid phase. A vapor pressure correlation and the critical pressure have also been derived from the experimental data.

Experimental Apparatus and Procedure

A constant-volume method was applied for measuring the vapor pressures and *PVT* properties of HCFC-123. Figure 1 shows the experimental apparatus, which is composed of a constant-volume cell immersed in a thermostated bath, a temperature-measurement device, a PID temperature controller, and a pressure-measurement device, etc. We have already measured *PVT* properties of 1,1,1,2-tetrafluoroethane (HFC-134a) (1), and perfluoro-2-methylpentane (2), with this apparatus.

The inner volume of the constant-volume cell was carefully calibrated by using the density of water and its volume change

Table I. Uncertainties of Data and Purities of Samples of HCFC-123

	series	$\Delta T /$ mK	purity/ wt %	$\Delta \rho /$ (kg·m ⁻³)	purity/ wt %
vapor pressures		±10	±2		99.8/99.82
<i>PVT</i> properties	a	±10	±2	±0.1	99.82
	b			±0.1	99.8
	c			±0.2	99.82
	d			±0.3	99.82
	e			±0.4	99.82
	f			±0.5	99.8
	g			±0.5	99.8
	h			±0.7	99.82
	i			±0.7	99.82
	j			±0.8	99.82
	k			±0.8	99.82
	l			±0.9	99.82
	m			±0.9	99.82
	n			±0.9	99.82
	o			±0.9	99.82
	p			±0.8	99.82
	q			±0.8	99.82
	r			±0.7	99.82
	s			±0.4	99.82

due to changes in temperature and pressure was calculated by using the thermal expansivity and Young's modulus of stainless steel. The volume was about 139 cm³ at room temperature. The density of the sample was determined from the inner volume of the cell and the mass of the sample confined in the cell, which was measured by a precision balance. The uncertainty of the cell volume was about ±0.02 to ±0.12%, depending on temperature and pressure, while the uncertainty of the sample mass was ±3 mg.

The temperature of silicon oil filled in a thermostated bath was controlled within ±3 mK by the PID temperature controller. At thermal equilibrium, which was confirmed by the pressure of the sample fluid in the cell being stable, the pressure and the temperature of the sample were measured.

The pressure of the sample was measured by the pressure gauges O1, O2, and O3 in Figure 1. The sample cell is connected with a differential pressure detector (B), which transfers the pressure of the sample to pressure-transfer medium, nitrogen gas. The mechanical behavior of the differential pressure detector (B) was calibrated before and after each series of measurements.

The temperature was measured with a standard platinum resistance thermometer (D in Figure 1), which was located near the sample cell. The platinum resistance thermometer was calibrated according to IPTS-68 at the National Laboratory of Metrology, Ibaraki, Japan.

* To whom correspondence should be addressed.

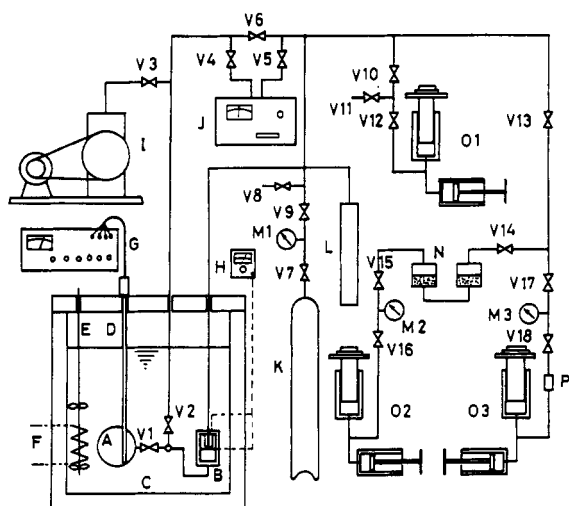


Figure 1. Experimental apparatus: (a) sample vessel, (B) differential pressure indicator, (C) thermostated bath, (D) platinum resistance thermometer, (E) stirrer, (F) heater, (G) bridge, (H) resistance meter, (I) vacuum pump, (J) precision Bourdon tube pressure gauge, (K) nitrogen bottle, (L) pressure damper, (M1–M3) pressure gauges, (N) oil-gas separator, (O1) air piston type pressure gauge (up to 0.4 MPa), (O2) oil piston type pressure gauge (up to 15.1 MPa), (O3) air piston type pressure gauge (1.1–15.1 MPa), (P) dust filter, (V1–V18) valves.

The experimental uncertainty in the temperature was estimated to be within ± 10 mK and ± 2.0 kPa in pressure. By considering the uncertainties of the volume of the sample cell and sample mass confined, the uncertainty of the density was estimated to be between ± 0.1 and 0.9 kg·m⁻³. The purity of the sample analyzed by the supplier was 99.8 and 99.82 wt %. The uncertainties and sample purities for each series of measurements are summarized in Table I.

Results

Vapor Pressures. Vapor pressures measured at temperatures from 308 K to the critical temperature are given in Table II. On the basis of these measurements, a vapor pressure equation that represents the experimental data within $\pm 0.26\%$ at temperatures above 308 K was established as follows:

$$\ln(P/P_c) = (a_1\tau + a_2\tau^{1.2} + a_3\tau^2 + a_4\tau^3)/(1 - \tau) \quad (1)$$

$$\tau = 1 - T_{68}/T_{c(68)}$$

$$a_1 = -7.87576 \quad a_2 = 1.45751 \quad a_3 = 0.520220$$

$$a_4 = -3.47970$$

$$P_c = 3.6655 \pm 0.0030 \text{ MPa} \quad T_{c(68)} = 456.86 \pm 0.02 \text{ K}$$

Table II gives the calculated values from eq 1 as P_{cal} , the deviations of the present data from P_{cal} , and the temperatures in ITS-90 as T_{90} , which were calculated from the temperatures of IPTS-68 as T_{68} .

Figure 2 shows the comparison of the measurements and correlating equations reported by Weber (3), Yamashita et al. (4), Fukushima et al. (5), Yamagishi and Oguchi (6), McLinden et al. (7), and the measurements of Morrison and Ward (8) with eq 1.

Equation 1 agrees with the previous measurements within $\pm 0.3\%$ except for those reported by Yamagishi and Oguchi (6), which show a large deviation from the others at temperatures below 320 K. It should be noted that the absolute pressure deviation of the data by Yamagishi and Oguchi (6) is less than 1.5 kPa. Equation 1 represents the present results with the standard deviation of 0.07% and the maximum deviation of 0.26%, the measurements of Weber (3) with 0.13 and 0.17%, the measurements of Yamashita et al. (4) with 0.10 and

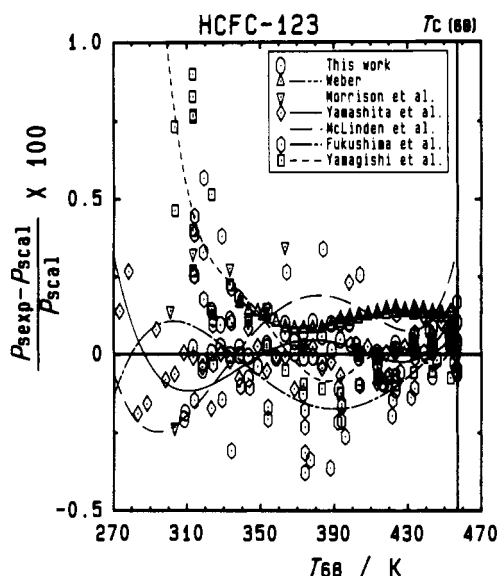


Figure 2. Percent vapor pressure deviations from eq 1.

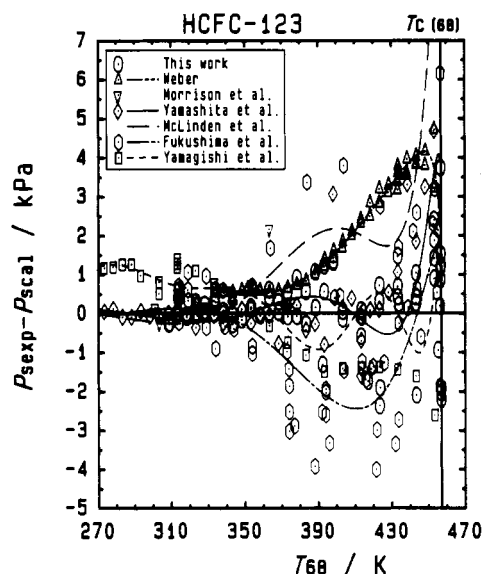


Figure 3. Absolute vapor pressure deviations from eq 1.

0.27%, the measurements of Fukushima et al. (5) with 0.21 and 0.57%, the measurements of Yamagishi and Oguchi (6) with 1.1 and 3.5%, and the measurements of Morrison and Ward (8) with 0.23 and 0.34%, respectively. Figure 3 shows the absolute pressure deviations of the above measurements from eq 1. Below the temperature of 350 K, eq 1 reproduces all of the measurements within ± 1.5 kPa, but for the region where the temperature is above 350 K, systematic deviations were found for each measurement.

The Critical Pressure. In the course of developing the vapor pressure correlation, the critical pressure was determined so as to coincide with the measured critical temperature and critical density reported by Tanikawa et al. (9). Along five isochores at densities of 530.1 ± 0.5 , 532.1 ± 0.5 , 554.7 ± 0.6 , 557.9 ± 0.7 , and 598.8 ± 0.7 kg·m⁻³ which encompass the critical density and two of them are within the critical density accompanied with the uncertainty observed by Tanikawa et al. (9), 556 ± 3 kg·m⁻³. The vapor pressures were measured at very small temperature intervals in the critical region, as shown in Figure 4 and Table II. On the basis of these experimental results, the vapor pressure correlation, eq 1, was developed, which fits the vapor pressures near the critical point very well. The critical pressure corresponding to the critical temperature $T_{c(68)} = 456.86 \pm 0.02$ K, measured by Tanikawa et al. (9),

Table II. Measured Vapor Pressures for HCFC-123 and Comparison with Values Calculated from Equation 1^a

no.	T_{68}/K	T_{90}/K	P_{exp}/MPa	P_{cal}/MPa	dev/%	no.	T_{68}/K	T_{90}/K	P_{exp}/MPa	P_{cal}/MPa	dev/%
1	308.27	308.26	0.131	0.131	-0.208	35	393.14	393.11	1.201	1.200	0.047
2	308.75	308.74	0.133	0.133	-0.187	36	398.12	398.09	1.326	1.324	0.099
3	312.98	312.97	0.154	0.154	0.022	37	398.13	398.10	1.326	1.325	0.102
4	313.53	313.52	0.157	0.156	0.255	38	403.15	403.11	1.459	1.459	0.003
5	318.14	318.13	0.182	0.182	-0.051	39	403.15	403.12	1.459	1.459	-0.010
6	318.14	318.13	0.182	0.182	-0.025	40	413.18	413.14	1.758	1.759	-0.033
7	323.13	323.11	0.212	0.212	0.006	41	413.19	413.16	1.759	1.759	0.005
8	323.13	323.12	0.213	0.212	0.140	42	416.76	416.73	1.874	1.876	-0.093
9	327.98	327.96	0.246	0.246	0.095	43	423.11	423.07	2.096	2.099	-0.113
10	328.13	328.12	0.247	0.247	0.025	44	423.14	423.11	2.100	2.100	0.015
11	333.14	333.12	0.286	0.286	0.112	45	423.16	423.12	2.101	2.100	0.035
12	333.14	333.12	0.286	0.286	-0.002	46	423.38	423.34	2.107	2.109	-0.090
13	338.13	338.11	0.329	0.329	-0.003	47	433.14	433.10	2.492	2.491	0.017
14	338.13	338.12	0.329	0.329	0.023	48	433.17	433.13	2.493	2.492	0.059
15	343.13	343.11	0.377	0.377	-0.006	49	433.18	433.15	2.494	2.493	0.028
16	343.14	343.12	0.377	0.378	-0.077	50	443.13	443.09	2.938	2.938	0.009
17	348.14	348.12	0.431	0.431	-0.040	51	443.14	443.10	2.939	2.939	0.014
18	353.13	353.11	0.490	0.490	0.034	52	443.16	443.12	2.940	2.939	0.035
19	353.13	353.11	0.490	0.490	0.022	53	443.18	443.14	2.938	2.941	-0.071
20	358.14	358.12	0.554	0.554	-0.011	54	453.12	453.08	3.452	3.451	0.041
21	363.13	363.10	0.626	0.625	0.100	55	453.12	453.08	3.452	3.451	0.026
22	363.14	363.12	0.626	0.625	0.066	56	453.15	453.11	3.454	3.452	0.054
23	368.16	368.13	0.703	0.703	0.042	57	453.17	453.13	3.456	3.454	0.070
24	368.19	368.17	0.703	0.703	0.003	58	455.17	455.13	3.565	3.566	-0.026
25	373.13	373.11	0.786	0.786	-0.011	59	456.14	456.10	3.623	3.623	0.005
26	373.14	373.11	0.787	0.787	0.070	60	456.17	456.13	3.623	3.624	-0.052
27	378.12	378.09	0.878	0.878	-0.009	61	456.52	456.48	3.646	3.645	0.024
28	378.18	378.15	0.880	0.880	0.105	62	456.55	456.51	3.648	3.647	0.032
29	383.14	383.11	0.978	0.977	0.058	63	456.57	456.53	3.646	3.648	-0.056
30	383.15	383.12	0.977	0.978	-0.028	64	456.62	456.58	3.652	3.651	0.033
31	388.13	388.10	1.085	1.084	0.098	65	456.65	456.61	3.654	3.653	0.042
32	388.41	388.38	1.091	1.091	0.014	66	456.68	456.64	3.658	3.655	0.102
33	392.15	392.12	1.175	1.177	-0.112	67	456.77	456.74	3.658	3.660	-0.052
34	393.13	393.10	1.201	1.200	0.101	68	456.77	456.74	3.658	3.660	-0.060

^a T_{68} = IPTS-68; T_{90} = ITS-90.

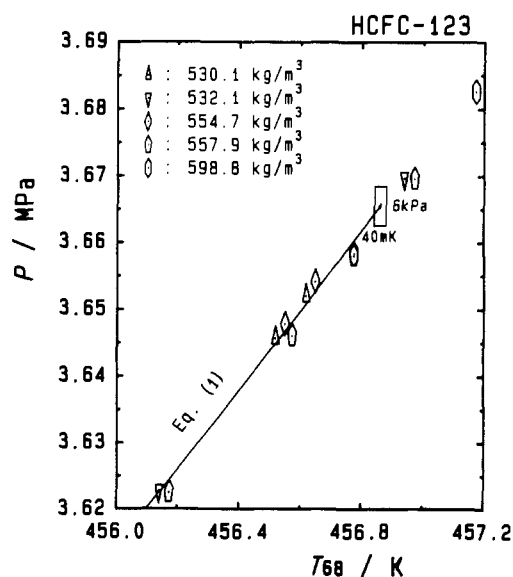


Figure 4. Vapor pressure measurements near the critical point of HCFC-123.

was finally determined as $P_c = 3.6655 \pm 0.0030$ MPa.

PVT Properties. The PVT properties of HCFC-123 were measured along 19 isochores in an extensive range of densities from 95 to 1440 $\text{kg}\cdot\text{m}^{-3}$, temperatures from 311 to 523 K, and pressures from 0.5 to 12 MPa, respectively. The 134 PVT measurements are listed in Table III, in both temperature scales of IPTS-68 and ITS-90 as T_{68} and T_{90} , respectively. The distribution of the present measurements in a temperature-density plane is illustrated in Figure 5.

So far, six experimental studies are available regarding the PVT properties of HCFC-123, i.e., those of Weber (3), Fuku-

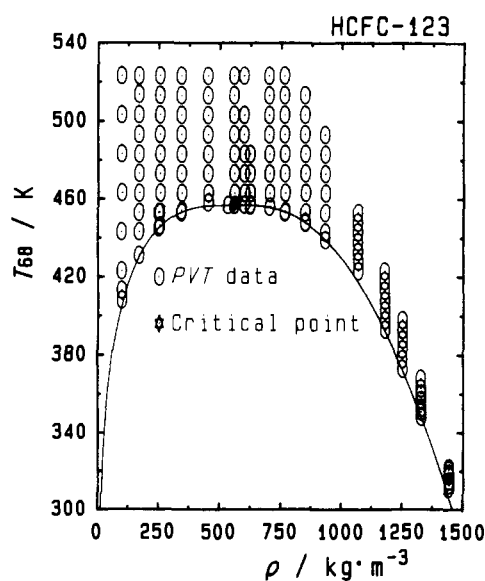


Figure 5. Distribution of the present PVT property data.

shima et al. (5), Yamagishi and Oguchi (6), Morrison and Ward (8), Maezawa et al. (10), and Matsuo (11). Figure 6 shows these measurements on a pressure-temperature plane with the present results. Matsuo (11) reported a set of PVT values up to 39 MPa in the liquid phase. Morrison and Ward (8) and Maezawa et al. (10) also reported the PVT measurements in the liquid region, while Weber (3) published a set of measurements in the gaseous phase. Fukushima et al. (5) and Yamagishi and Oguchi (6) reported the PVT measurements in the limited range of gaseous and liquid phase, whereas the present

Table III. PVT Measurements for HCFC-123^a

no.	T_{68}/K	T_{90}/K	P/MPa	$\rho/(kg\cdot m^{-3})$	no.	T_{68}/K	T_{90}/K	P/MPa	$\rho/(kg\cdot m^{-3})$	no.	T_{68}/K	T_{90}/K	P/MPa	$\rho/(kg\cdot m^{-3})$
a Series				h Series				n Series						
1	408.16	408.12	1.540	95.98	48	456.97	456.93	3.670	557.9	94	439.17	439.13	2.781	931.0
2	413.16	413.13	1.577	95.96	49	463.17	463.14	4.046	557.7	95	443.17	443.13	3.408	930.8
3	423.16	423.13	1.650	95.91	50	473.18	473.14	4.662	557.5	96	453.17	453.13	5.051	930.3
4	443.17	443.13	1.791	95.83	51	483.18	483.14	5.287	557.2	97	463.18	463.14	6.737	929.9
5	463.18	463.14	1.930	95.73	52	493.18	493.14	5.917	556.9	98	473.17	473.13	8.448	929.4
6	483.18	483.14	2.062	95.64	53	503.19	503.14	6.548	556.6	99	483.18	483.14	10.178	928.9
7	503.18	503.14	2.192	95.55	54	513.19	513.15	7.180	556.3	100	493.18	493.14	11.929	928.4
8	523.19	523.15	2.320	95.45	55	523.19	523.15	7.813	556.0	o Series				
b Series				i Series				p Series						
9	431.11	431.08	2.376	167.8	56	457.17	457.13	3.683	598.8	101	423.17	423.13	3.333	1066.7
10	443.13	443.09	2.555	167.7	57	463.18	463.14	4.075	598.6	102	428.16	428.13	4.570	1066.4
11	453.14	453.10	2.698	167.6	58	473.18	473.14	4.752	598.3	103	433.17	433.13	5.824	1066.1
12	463.15	463.11	2.837	167.5	59	483.18	483.14	5.443	598.0	104	438.17	438.13	7.108	1065.9
13	473.14	473.10	2.972	167.4	60	493.18	493.14	6.141	597.7	105	443.17	443.13	8.342	1065.6
14	483.15	483.11	3.106	167.3	61	503.18	503.14	6.845	597.4	106	448.17	448.13	9.607	1065.3
15	493.16	493.12	3.231	167.3	62	523.19	523.15	8.260	596.8	107	453.17	453.13	10.878	1065.0
16	503.18	503.14	3.367	167.2	j Series				q Series					
17	513.61	513.57	3.501	167.1	63	456.68	456.64	3.658	623.2	108	393.27	393.24	1.414	1175.6
18	523.14	523.10	3.621	167.0	64	457.18	457.14	3.691	623.1	109	398.16	398.12	3.087	1175.3
c Series				k Series				r Series						
19	445.22	445.18	3.024	249.1	65	463.18	463.14	4.102	623.0	110	403.16	403.13	4.809	1175.0
20	453.17	453.13	3.222	249.0	66	473.18	473.14	4.815	622.6	111	408.16	408.12	6.536	1175.0
d Series				l Series				s Series						
21	446.26	446.22	3.066	254.4	68	456.17	456.13	3.639	701.5	112	413.16	413.13	8.266	1174.3
22	453.16	453.12	3.241	254.3	69	463.17	463.13	4.216	701.2	113	418.16	418.13	10.002	1174.0
23	463.18	463.14	3.497	254.2	70	473.18	473.14	5.085	700.9	114	423.16	423.13	11.737	1173.7
24	473.18	473.14	3.721	254.0	71	483.18	483.14	5.980	700.5	t Series				
25	483.18	483.14	3.945	253.9	72	493.18	493.14	6.890	700.2	115	373.15	373.12	1.195	1248.9
26	493.18	493.14	4.169	253.8	73	503.18	503.14	7.815	699.8	116	378.15	378.12	3.339	1248.5
27	503.18	503.14	4.387	253.7	74	513.19	513.15	8.744	699.4	117	383.15	383.12	5.485	1248.2
28	513.19	513.15	4.597	253.5	75	523.19	523.15	9.680	699.1	118	388.15	388.12	7.655	1247.8
29	523.19	523.15	4.803	253.4	m Series				u Series					
e Series				n Series				v Series						
30	453.18	453.14	3.443	342.3	76	453.17	453.13	3.456	764.6	121	348.34	348.32	0.524	1324.7
31	454.06	454.02	3.476	342.3	77	453.67	453.64	3.502	764.5	122	351.14	351.12	2.032	1324.5
32	463.17	463.13	3.805	342.1	78	463.18	463.14	4.438	764.2	123	353.14	353.12	3.109	1324.3
33	473.19	473.15	4.152	342.0	79	473.18	473.14	5.474	763.8	124	357.14	357.12	5.260	1324.0
34	483.19	483.15	4.489	341.8	80	483.18	483.14	6.539	763.4	125	360.43	360.41	7.030	1323.8
35	493.19	493.15	4.819	341.6	81	493.18	493.14	7.622	763.0	126	363.14	363.12	8.486	1323.6
36	503.19	503.15	5.146	341.4	82	503.18	503.14	8.718	762.6	127	368.15	368.12	11.173	1323.2
37	513.19	513.15	5.468	341.3	83	513.19	513.15	9.824	762.2	w Series				
38	523.19	523.15	5.787	341.1	84	523.19	523.15	10.938	761.8	128	311.28	311.28	3.429	1439.5
f Series				o Series				x Series						
39	458.24	458.20	3.727	451.2	85	447.77	447.73	3.176	848.4	129	313.14	313.13	4.834	1439.3
40	463.12	463.08	3.969	451.1	86	448.17	448.13	3.223	848.4	130	315.14	315.13	6.340	1439.2
41	473.17	473.13	4.455	450.9	87	453.17	453.13	3.844	848.2	131	318.14	318.12	8.614	1438.9
42	483.14	483.10	4.931	450.6	88	463.18	463.14	5.132	847.8	132	319.14	319.13	9.366	1438.8
43	493.15	493.11	5.406	450.4	89	473.18	473.14	6.462	847.3	133	321.14	321.13	10.870	1438.7
44	503.13	503.09	5.875	450.2	90	483.20	483.16	7.817	846.9	134	322.14	322.12	11.624	1438.6
45	513.13	513.09	6.343	449.9	91	493.18	493.14	9.190	846.4	y Series				
46	523.15	523.11	6.810	449.7	92	503.18	503.14	10.576	846.0	135	311.28	311.28	3.429	1439.5
g Series				z Series				aa Series						
47	456.94	456.90	3.670	532.1	93	513.19	513.15	11.968	845.5	136	313.14	313.13	4.834	1439.3

^a T_{68} = IPTS-68; T_{90} = ITS-90.

measurements cover a wide range of the conditions in the entire fluid phase, as shown in Figure 6.

Discussion

Since the first thermodynamic property studies of HCFC-123 started only 3 years ago, only a single equation of state reported by McLinden et al. (7) is available for HCFC-123 at present. This equation of state was developed mainly on the basis of PVT measurements by Weber (3) in the gaseous phase. The comparison of the available PVT data with that equation of state is shown in Figures 7 and 8. Below a density of $200\text{ kg}\cdot\text{m}^{-3}$, the equation represents the present data, the

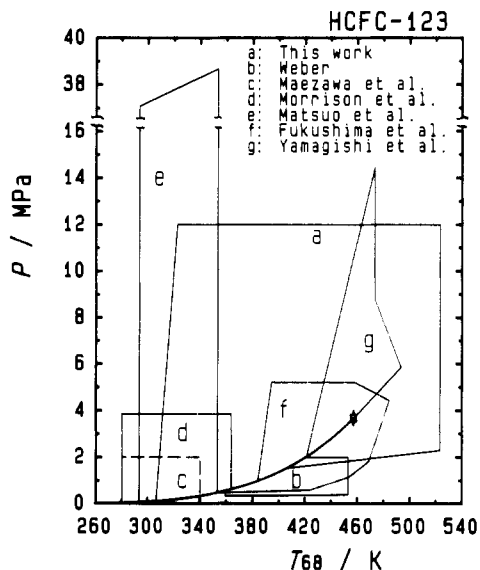
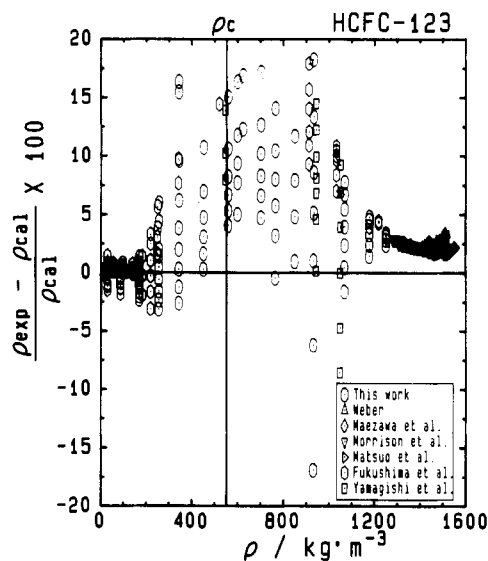
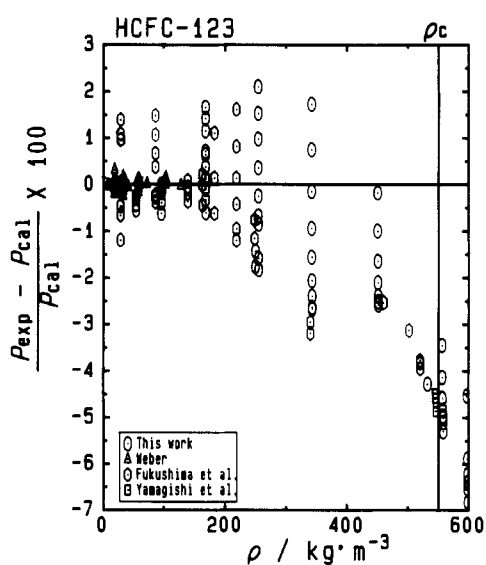
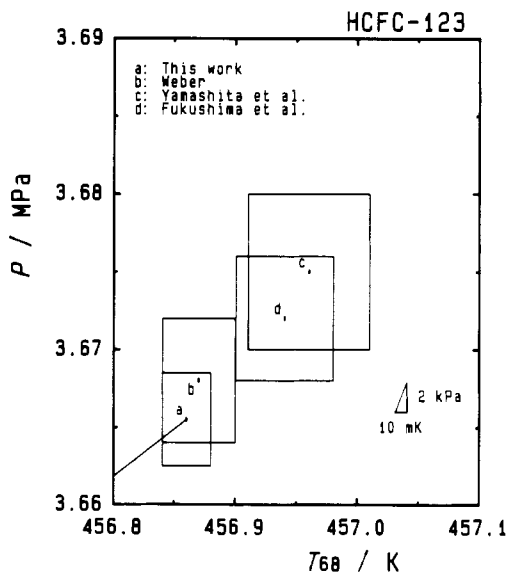
measurements of Weber (3), and those of Fukushima et al. (5) very well, but above $200\text{ kg}\cdot\text{m}^{-3}$ the equation does not reproduce the measurements.

Concerning the critical parameters, four reports are available beside the present study for HCFC-123, which are listed in Table IV. The reported values of the critical pressure and temperature together with the claimed uncertainties are summarized in Figure 9. A set of the critical temperature observed by Tanikawa et al. (9) and the critical pressure by the present authors agrees well with that of Weber (3). On the other hand, the critical parameters reported by Yamashita et al. (4) and Fukushima et al. (5) agree with each other, although their values differ from the present results by more than the mutual estimated uncertainties.

Table IV. Critical Parameters of HCFC-123^a

first author	year	$T_{c(68)}/K$	$T_{c(90)}/K$	$\Delta T_c/K$	P_c/MPa	$\Delta P_c/MPa$	$\rho_c/(kg \cdot m^{-3})$	$\Delta \rho_c/(kg \cdot m^{-3})$	purity/wt %	ref no.
Tanikawa	1989	456.86	456.82	± 0.02	3.675	± 0.005	556	± 3	99.8/99.99	9
Yamashita	1989	456.96	456.92	± 0.05	3.675	± 0.005	556	± 3	99.5	4
Fukushima	1990	456.94	456.90	± 0.04	3.672	± 0.004	553	± 5	99.8/99.9	5
Weber	1990	456.87	456.83	± 0.03	3.668	± 0.004	550	± 4	99.95	3
this work	1990	456.86 ^b	456.82 ^b	± 0.02 ^b	3.6655	± 0.0030	556 ^b	± 3 ^b	99.8/99.82	

^aScales used: $T_{c(68)}$, IPTS-68; $T_{c(90)}$, ITS-90. ^bValues reported by Tanikawa et al. (9).

**Figure 6.** Measured ranges of the PVT property data for HCFC-123.**Figure 8.** Density deviation from the equation of state developed by McLinden et al. (7).**Figure 7.** Pressure deviation from the equation of state developed by McLinden et al. (7).**Figure 9.** Comparison of the critical parameters associated with the claimed uncertainties.

Conclusion

An extensive set of *PVT*, vapor pressure, and the critical parameters of HCFC-123 has been measured. The present experimental *PVT* measurements are the first set covering a wide range of the state parameters in the entire fluid phase. Vapor pressures and the critical pressure have also been reported with high reliability, i.e., ± 2 and ± 3 kPa, respectively. A vapor pressure correlation was developed which is considered effective in the temperature range from 300 K to the critical temperature, although it may be extrapolated to the lowest temperature of 270 K.

Acknowledgment

We thank the following undergraduate students at Keio University for their assistance: Tomihiro Oda, Kazuhiko Murakami, and Minoru Uchida. We are also grateful to Ashahi Glass Co. Ltd. for furnishing the sample and to Toray Silicone Co. Ltd. for furnishing the silicon oil.

Registry No. $CHCl_2CF_3$, 306-83-2.

Literature Cited

- (1) Piao, C.-C.; Sato, H.; Watanabe, K. *ASHRAE Trans.* **1990**, *96* (1), 132.

- (2) Momoda, K.; Uematsu, M.; Watanabe, K. *Ber. Bunsen-Ges. Phys. Chem.* **1984**, *88*, 1007.
 (3) Weber, L. A. *J. Chem. Eng. Data* **1990**, *35*, 237.
 (4) Yamashita, T.; Kubota, H.; Tanaka, Y.; Makita, T.; Kashiwagi, H. *Proc. 10th Jpn. Symp. Thermophys. Properties* **1989**, 75.
 (5) Fukushima, M.; Watanabe, N.; Kamimura, T. *Trans. Jpn. Assoc. Refrig.* **1990**, *7* (3), 243.
 (6) Yamagishi, M.; Oguchi, K. *Proc. 31st High Pressure Conf. Jpn.* **1990**, 12.
 (7) McLinden, M. O.; Gallagher, J. S.; Weber, L. A.; Morrison, G.; Ward, D.; Goodwin, A. R. H.; Moldover, M. R.; Schmidt, J. W.; Chae, H. B.; Bruno, T. J.; Ely, J. F.; Huber, M. L. *ASHRAE Trans.* **1989**, *95* (2), 263.
 (8) Morrison, G.; Ward, D. K. *Fluid Phase Equil.*, in press.
 (9) Tanikawa, S.; Kabata, Y.; Sato, H.; Watanabe, K. *J. Chem. Eng. Data* **1990**, *35*, 381.
 (10) Maezawa, Y.; Sato, H.; Watanabe, K. *J. Chem. Eng. Data* **1990**, *35*, 225.
 (11) Matsuo, S. Kobe University Japan, private communication, Oct 1990.

Received for review December 11, 1990. Accepted May 29, 1991. The financial support of the Grants-in-Aid for Scientific Research Fund in 1988 and 1989 (Project No. 63603024 and No. 01603022) by the Ministry of Education, Science and Culture, Japan, is gratefully acknowledged.

Apparent and Partial Molal Volumes of Selected Symmetrical Tetraalkylammonium Bromides in 2-Methoxy-1-ethanol at 25 °C

Bljan Das and Dilip K. Hazra*

Department of Chemistry, North Bengal University, 734430 Darjeeling, India

The apparent and partial molal volumes of six symmetrical tetraalkylammonium bromides, R_4NBr ($R = C_2H_5$ to C_7H_{15}) in 2-methoxy-1-ethanol (ME) have been determined at 25 °C. The limiting apparent molal volumes (ϕ_v°) and the experimental slopes (S_v°) have been interpreted in terms of ion-solvent and ion-ion interactions, respectively. Use has been made of the nonthermodynamic, so-called extrapolation method to split the limiting apparent molal volumes into ionic contributions. The $\bar{V}_{R,NX}^\circ$ values in 2-methoxy-1-ethanol are found to be almost similar to those in other organic solvents examined and differ greatly from the values in water and heavy water solutions. The ion-solvent interaction effect, as estimated by the combination of the viscosity B_{ion} values with \bar{V}_{ion}° values, indicates that these ions may be classified as "structure breakers" in this solvent medium.

Introduction

The volumetric behavior of solutes has proved to be very useful in elucidating the various interactions occurring in aqueous and nonaqueous solutions (1). Studies on the apparent and partial molal volumes of electrolytes have been used to examine the ion-ion, ion-solvent, and solvent-solvent interactions (2). The apparent and partial molal volumes of tetraalkylammonium salts have been investigated rather extensively in aqueous (3-5) and nonaqueous solutions (6, 7). Such measurements have also been reported for water-organic solvent binary systems (8). However, no work has been reported on the apparent and partial molal volumes of tetraalkylammonium bromides, R_4NBr ($R = C_2H_5$ to C_7H_{15}) in 2-methoxy-1-ethanol at 25 °C. 2-Methoxy-1-ethanol is a "quasi-aprotic" solvent (9) of low dielectric constant ($\epsilon_{25^\circ C} = 16.93$). In recent years much attention has been given to this solvent, since it is of particular interest in the field of various industrial processes, synthesis, and electrochemical studies (10, 11).

Experimental Section

2-Methoxy-1-ethanol (G.R.E. Merck) was distilled twice in an all-glass distillation set immediately before use. The purified solvent had a density of 0.960 02 g cm⁻³, a coefficient of viscosity of 1.5414 cP, and a specific conductance of ca. $1.01 \times 10^{-8} \Omega^{-1} \text{cm}^{-1}$ at 25 °C. These values are in good agreement with the literature values (12), 0.960 24 g cm⁻³, 1.60 cP,

and $1.09 \times 10^{-8} \Omega^{-1} \text{cm}^{-1}$ (at 20 °C), respectively.

Tetraalkylammonium bromides were of Fluka purum or puriss grade; these were purified as described in the literature (13) and also described earlier by us (14). The salts were purified by recrystallization, and the higher homologues were recrystallized twice to ensure highest purity. The recrystallized salts were dried under vacuum at elevated temperatures for 12 h. The salts were stored in a vacuum desiccator and dried for 3-4 h at 100 °C prior to use.

A stock solution for each salt was prepared by weight, and working solutions in the concentration range $0.01 < c/(\text{mol dm}^{-3}) < 0.12$ were obtained by weight dilution. The conversion of the molality into molarity was done by using the density values. The densities were measured with an Ostwald-Sprengel type pycnometer having a bulb volume of about 25 cm³ and an internal diameter of the capillary of about 1 mm. The pycnometer was calibrated at 25 °C with doubly distilled water. Measurements were made in an oil bath maintained at 25 ± 0.005 °C by means of a mercury-in-glass thermoregulator, and the absolute temperature was determined by a calibrated platinum resistance thermometer and Muller bridge. The precision of the density measurements was greater than $\pm 3 \times 10^{-5} \text{g cm}^{-3}$.

Results and Discussion

The apparent molal volumes, ϕ_v , of the solutes were calculated from the densities of the solutions by using the equation

$$\phi_v = M/\rho_0 - 1000(\rho - \rho_0)/c\rho_0 \quad (1)$$

where M is the molecular weight of the solute, ρ_0 and ρ are the densities of the solvent and the solution, respectively, and c is the concentration in molarity.

The partial molal volumes, \bar{V}_2 , were computed from ϕ_v with the equation

$$\bar{V}_2 = \phi_v + \frac{1000 - c\phi_v}{2000 + c^{3/2}(\partial\phi_v/\partial c^{1/2})} c^{1/2}(\partial\phi_v/\partial c^{1/2}) \quad (2)$$

The molar concentrations, densities, and apparent and partial molal volumes of the solutions of various tetraalkylammonium bromides in 2-methoxy-1-ethanol at 25 °C are reported in Table I. The limiting apparent molal volumes, ϕ_v° (equal to the partial molal volumes at infinite dilution, \bar{V}_2°), were obtained by least-squares fitting of ϕ_v values to the equation

$$\phi_v = \phi_v^\circ + S_v^\circ c^{1/2} \quad (3)$$